Development/Plasticity/Repair

PIP_3 Regulates Spinule Formation in Dendritic Spines during Structural Long-Term Potentiation

Yoshibumi Ueda[1,2] **and Yasunori Hayashi**[1,2,3]

[1]Brain Science Institute, RIKEN, Wako, Saitama 351-0198, Japan, [2]RIKEN-MIT Neuroscience Research Center, The Picower Institute for Learning and Memory, Department of Brain and Cognitive Sciences, Massachusetts Institute of Technology, Cambridge, Massachusetts 02139, and [3]Saitama University Brain Science Institute, Saitama University, Saitama 338-8570, Japan

Dendritic spines are small, highly motile structures on dendritic shafts that provide flexibility to neuronal networks. Spinules are small protrusions that project from spines. The number and the length of spinules increase in response to activity including theta burst stimulation and glutamate application. However, what function spinules exert and how their formation is regulated still remains unclear. Phosphatidylinositol-3,4,5-trisphosphate (PIP_3) plays important roles in cell motility such as filopodia and lamellipodia by recruiting downstream proteins such as Akt and WAVE to the membrane, respectively. Here we reveal that PIP_3 regulates spinule formation during structural long-term potentiation (sLTP) of single spines in CA1 pyramidal neurons of hippocampal slices from rats. Since the local distribution of PIP_3 is important to exert its functions, the subcellular distribution of PIP_3 was investigated using a fluorescence lifetime-based PIP_3 probe. PIP_3 accumulates to a greater extent in spines than in dendritic shafts, which is regulated by the subcellular activity pattern of proteins that produce and degrade PIP_3. Subspine imaging revealed that when sLTP was induced in a single spine, PIP_3 accumulates in the spinule whereas PIP_3 concentration in the spine decreased.

Introduction

Spinules are filopodia-like protrusion structures, which are commonly observed on spines. Electron microscopy data show that spinules exist on 32% of spines under basal conditions (Spacek and Harris, 2004). The number of spinules increases in response to stimuli such as theta burst stimulation (Toni et al., 1999), local glutamate stimulation (Richards et al., 2005), and high potassium application (Tao-Cheng et al., 2009). Several proposals for the biological significance of spinules have been made. Spinules extend toward a stimulation site upon local glutamate application (Richards et al., 2005). Tetrodotoxin (TTX) treatment causes spinules to move toward functional presynaptic boutons and contribute to the formation of new synapses (Richards et al., 2005). Additionally, spinules are sometimes engulfed by presynaptic axons. Furthermore, coated pits are present on the tips of these spinules, indicating that spinules are endocytosed (Spacek and Harris, 2004). Endocytosed-spinules are sometimes observed in presynaptic buttons as isolated vesicles separated from the postsynaptic side. (Spacek and Harris, 2004). Therefore, the *trans*-endocytosis of spinules may serve as a mechanism for retrograde signaling or may aid postsynaptic membrane remodeling by removing the excess membrane between postsynaptic sites (Spacek and Harris, 2004).

Phosphatidylinositol-3,4,5-trisphosphate (PIP_3) is a lipid second messenger that plays important roles in a diverse range of neuronal functions. The basal level of PIP_3 is crucial for maintaining AMPA receptor clustering during long-term potentiation (LTP; Arendt et al., 2010). As well as functional LTP, PIP_3 also regulates different aspects of cell polarity such as dendritic arborization and nerve growth factor-induced axonal filopodia formation (Jaworski et al., 2005; Ketschek and Gallo, 2010). To exert these functions, local PIP_3 accumulation is thought to be important and leads to the recruitment of effector proteins such as Akt (Thomas et al., 2001), WAVE (Oikawa et al., 2004), and guanine nucleotide exchange factors of small G-proteins to specific subcellular compartments (Han et al., 1998; Shinohara et al., 2002; Innocenti et al., 2003). However, the subcellular distribution of PIP_3 in neurons remains poorly understood.

In the present study, we found that PIP_3 regulates the number of spinules during the structural expansion of spines, designated here as sLTP. To study the local distribution of PIP_3, a fluorescence lifetime-based PIP_3 probe, FLIMPA3, was constructed. PIP_3 showed greater accumulation in spines than in dendritic shafts under basal conditions. Whereas PIP_3 concentration in a given spine decreased during the glutamate-induced enlargement of a spine, PIP_3 concentration in spinules increased. Accumulated PIP_3 in spinules may work as a retrograde signaling factor or may be involved in new synapse formation.

Received July 2, 2012; revised May 4, 2013; accepted May 28, 2013.

Author contributions: Y.U. and Y.H. designed research; Y.U. performed research; Y.U. analyzed data; Y.U. and Y.H. wrote the paper.

This work was supported by a Grant-in-Aid for Young Scientists (B) and the Special Postdoctoral Researcher Program of RIKEN (Y.U.) and by RIKEN, National Institutes of Health Grant R01DA17310, Grant-in-Aid for Scientific Research (A), and Grant-in-Aid for Scientific Research on Innovative Area "Foundation of Synapse and Neurocircuit Pathology" from the Ministry of Education, Culture, Sports, Science and Technology, Japan (Y.H.). We thank L. Yu, M. Bosch, S. Kwok, F. Hullin-Matsuda, T. Saneyoshi, T. Hosokawa, K. Mizuta, and K. Kim for valuable comments. We are also grateful to A. Suzuki, M. Kawano, H. Matsuno, and K. Matsuura for the preparation of hippocampal slices.

Correspondence should be addressed to Dr. Yoshibumi Ueda, Brain Science Institute, RIKEN, 2-1 Hirosawa, Wako, Saitama 351-0198, Japan. E-mail: yueda@riken.jp or happyvybecool@gmail.com.

DOI:10.1523/JNEUROSCI.3122-12.2013

 0270-6474/13/3311040-08$15.00/0

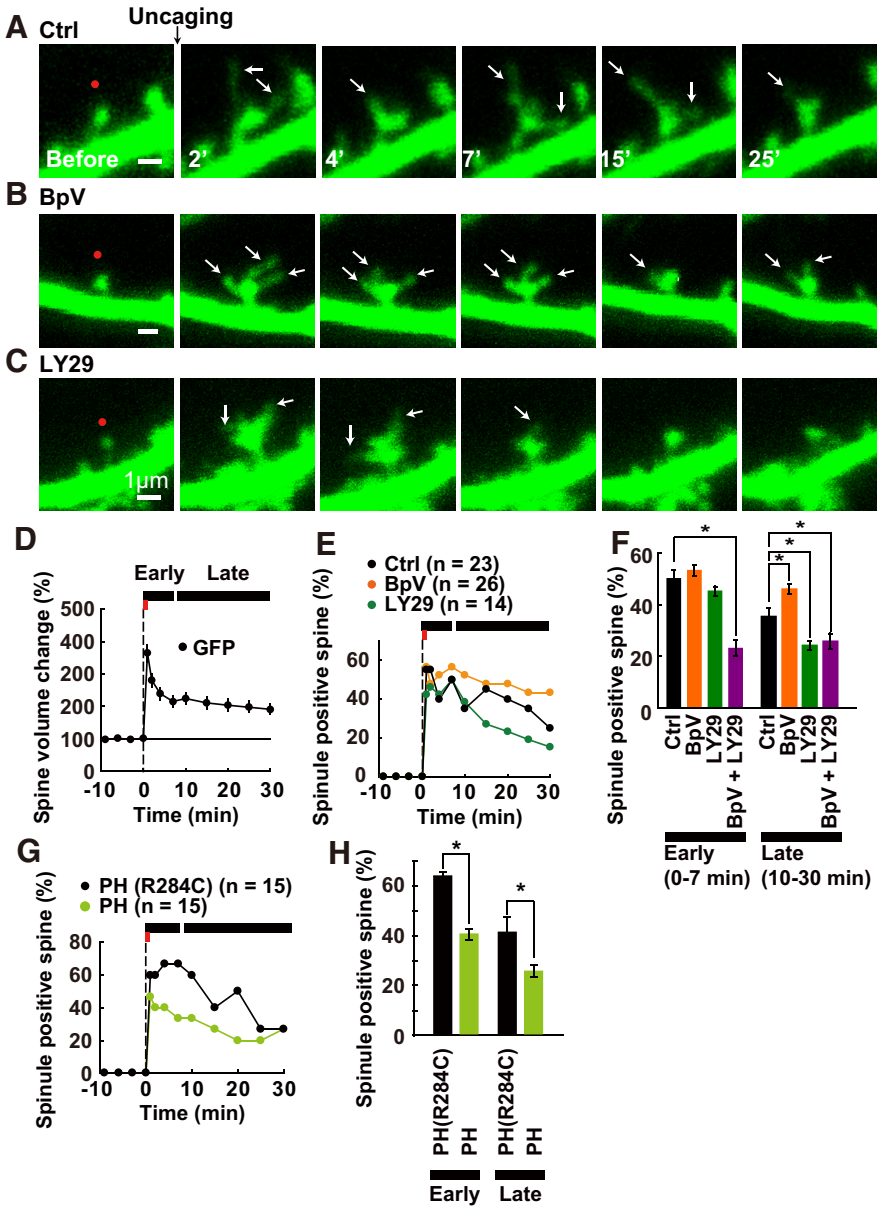

Figure 1. Effect of PIP_3 levels on spinule formation in spines induced by sLTP. ***A–C***, The effect of PIP_3 levels on spinule formation during sLTP using glutamate uncaging (Ctrl 0.4% DMSO; ***A***), a PTEN inhibitor–1 μM BpV(HOpic; ***B***), and a PI3K inhibitor, 30 μM LY294002 (***C***). Each drug was added over 30 min before induction of sLTP. Red spots on baseline images indicate the points that were subjected to glutamate uncaging. Spinules are indicated by arrows. Scale bar, 1 μm. ***D***, Time course of the enlargement of GFP-expressing spines following the induction of sLTP. The red bar indicates the time period of glutamate uncaging. First and second black bars indicate early (0–7 min) and (10–30 min) late phases, respectively. ***E***, Time course of the formation of spinule-positive spines; n = the number of spines subjected to glutamate uncaging. ***F***, The occurrence of spinule-positive spines in early and late phases in the presence of each drug. Asterisks denote a statistically significant difference ($p < 0.05$) from the value in the spine that was subjected to sLTP. ***G***, ***H***, The effect of PH domain on spinule formation. mCherry-PH and mCherry-PH (R284C) were overexpressed with mEGFP as a volume marker.

Materials and Methods

Constructs. Monomeric enhanced green fluorescent protein (mEGFP), the fluorescent resonance energy transfer (FRET) donor, was prepared by introducing a single point mutation (A206K) to EGFP. sREACh, the FRET acceptor, was made as previously described (Murakoshi et al., 2008). For the FLIMPA3 probe, the cyan fluorescent protein (CFP) and yellow fluorescent protein (YFP) of the FRET-based PIP_3 probe (Sato et al., 2003) were exchanged with mEGFP and sREACh respectively. The pleckstrin homology (PH) domain was from human GRP1. In the FLIMPA3 mutant, amino acids R284 and K343 were, respectively, mutated to a cysteine and alanine residue to abolish PIP_3 binding. For the experiment where the PH domain was overexpressed, a PH domain from rat GRP1 was used (a gift from Dr. José A. Esteban; Arendt et al., 2010). A single point mutation was introduced by PCR-directed mutagenesis to create PH (R284C), which abolished PIP_3 binding. PH and PH (R284C) were cloned downstream of mCherry. All constructs were driven by the CAG promoter.

Reagents. TTX was from Latoxan. Picrotoxin was from Nacalai Tesque. BpV(HOpic) was from Calbiochem. LY294002 was from Cayman Chemical Company. 4-Methoxy-7-mitroindolinyl (MNI)-L-glutamate was from Tocris Bioscience. Phospho-Akt (Ser473) antibody was from Cell Signaling Technology.

Neuronal slice culture and probe expression. Organotypic slice cultures of rat hippocampus of either sex were prepared from postnatal day 6–8 rats in accordance with the animal care and use guidelines of RIKEN. Slices were biolistically transfected after 5–8 d *in vitro* with FLIMPA3. Imaging was performed 1 d after transfection in the distal part of the main apical dendritic shafts of CA1 pyramidal neurons.

Culture of Chinese hamster ovary cells and probe expression. Chinese hamster ovary (CHO) cells were cultured in Ham's F12 Nutrient Mixture (Life Technologies), supplemented with 10% fetal calf serum and 1% penicillin/streptomycin at 37°C in 5% CO_2. FLIMPA3, FLIMPA3 mutant, and PH domain were transfected with Lipofectamine 2000 (Life Technologies) according to the manufacture's instruction, and left for 24 h at 37°C in 5% CO_2. We sometimes observed FLIMPA3 and FLIMPA mutant localized at the intracellular membrane of CHO cells possibly due to leak. Therefore, we cannot totally rule out that our spine images may also include signal from the intracellular pool of PIP_3.

Observation of Akt activity. CHO cells were plated onto glass dishes. FLIMPA3, FLIMPA3 mutant, and PH domain were transfected with Lipofectamine 2000 and left for 24 h at 37°C in 5% CO_2. One day after transfection, cells were treated with 50 ng/ml platelet-derived growth factor (PDGF) for 30 min, fixed with 4% paraformaldehyde for 20 min at room temperature, incubated with 50 mM NH_4Cl for 5 min, and then washed with PBS(−) twice. The cells were treated with PBS containing 0.2% Triton X-100 for 5 min, followed by treatment with blocking buffer (PBS/5% normal goat serum/0.1% Triton X-100) for 1.5 h. Then, anti-serine 473 rabbit antibody (1:25) in blocking buffer was applied at 4°C overnight. The cells were washed with PBS twice and incubated with goat anti-rabbit antibody conjugated with Alexa Fluor 555 in PBS(−) (1:250) for 2 h. Images were acquired using an Olympus FV1000 confocal microscopy. Immunostaining signal on the plasma membrane was measured by drawing a line profile across the cells using ImageJ software.

Two-photon imaging. Slices were maintained in a continuous perfusion of modified artificial CSF (ACSF) containing the following (in mM): 119 NaCl, 2.5 KCl, 3 $CaCl_2$, 26.2 $NaHCO_3$, 1 NaH_2PO_4, and 11 glucose, bubbled and equilibrated with 5% CO_2/95% O_2. Then 1 μM TTX, 50 μM picrotoxin, and 2.5 mM MNI-glutamate were added to the solution.

Time-lapse imaging was performed using a two-photon microscope (Fluoview 1000; Olympus) equipped with a Mai Tai laser (Sprectra-Physics; Newport). All imaging experiments were performed at 30°C. We always make comparisons among datasets recorded in an interleaved manner. In neurons expressing mEGFP, *Z*-stacks of 15–17 sections separated by 0.5 μm were summed. A constant region of interest was outlined around the spine and the total integrated fluorescence intensity of the green channel was calculated using ImageJ (by W.S. Rasband; National Institutes of Health, Bethesda, MD). Values were background-subtracted.

Fluorescence lifetime imaging. FLIMPA3 was excited at 910 nm and fluorescence levels were detected with a PMT (H7422P-40; Hamamatsu) that was located after the wavelength filters (Chroma Technology, HQ510/70–2p for GFP and BrightLine multiphoton filter 680SP). Fluorescence lifetime images were produced on a PCI board (SPC-730 and 830; Becker-Hickl). SPC images (Becker-Hickl) were used for constructing fluorescence lifetime images.

LTP induction by two-photon glutamate uncaging. Two-photon uncaging of MNI-glutamate was performed with a Mai Tai laser (Sprectra-Physics) tuned to 720 nm. A repetitive pattern of 2 ms pulses (4–5 mW) at 1 Hz for 30 s (Fig. 1*A–F*), 40 s (Fig. 1*G*,*H*), or 1 min (Fig. 5) was used to induce LTP at the targeted spine.

Synaptic spinule counts. Spinules that protruded from the spine head were counted. Each synaptic spinule, regardless of size and orientation, was scored as in previous studies (Tao-Cheng et al., 2009).

Statistics. All values are expressed as mean ± SEM. Statistical analysis was performed using Student's *t* test.

Results

To investigate how spinule formation occurs during sLTP, GFP was expressed in CA1 pyramidal neurons of organotypic hippocampal slices. First, spine size was investigated by observing GFP intensity. When local glutamate stimulation was induced at single dendritic spines using two-photon uncaging of MNI-caged glutamate, the spines rapidly enlarged after the stimulation and then shrank to a certain extent. However, the spine size was persistently larger at 30 min after stimulation than before the stimulation (Fig. 1*D*). The time course of spine enlargement is consistent with a previous report (Matsuzaki et al., 2004), and indicates that sLTP was successfully induced. During sLTP, we often observed the generation of filopodia-like protrusion structures termed spinules. The incidence of spinule occurrence increased quickly after glutamate uncaging, and then gradually decreased over time (Fig. 1*A*,*E*,*F*).

Considering that PIP_3 regulates the motility of cellular structures, we hypothesized that PIP_3 could modulate spinule formation on spines during sLTP. Therefore, we examined the effect of PIP_3 on spinule formation after glutamate stimulation. Application of BpV(HOpic), an inhibitor for phosphatase and tensin homolog (PTEN; an enzyme that degrades PIP_3 to phosphatidylinositol-4,5-bisphosphate, PIP_2) (Jurado et al., 2010), increased the number of spinules during the late phase of sLTP (Fig. 1*B*,*E*,*F*). The effect of PTEN inhibitor was abolished by pretreatment with LY294002, an inhibitor for phosphatidylinositol 3-kinase (PI3K; the enzyme that produces PIP_3), in both early and late phases (Fig. 1*F*). PTEN has both PIP_3 phosphatase activity and protein phosphatase activity for Shc and focal adhesion kinase (Gu et al., 1999). These data show that the increase in spinule formation was caused by an increase in PIP_3 rather than inhibition of protein dephosphorylation. Pretreating cells with LY294002 alone lead to a decrease in the number of

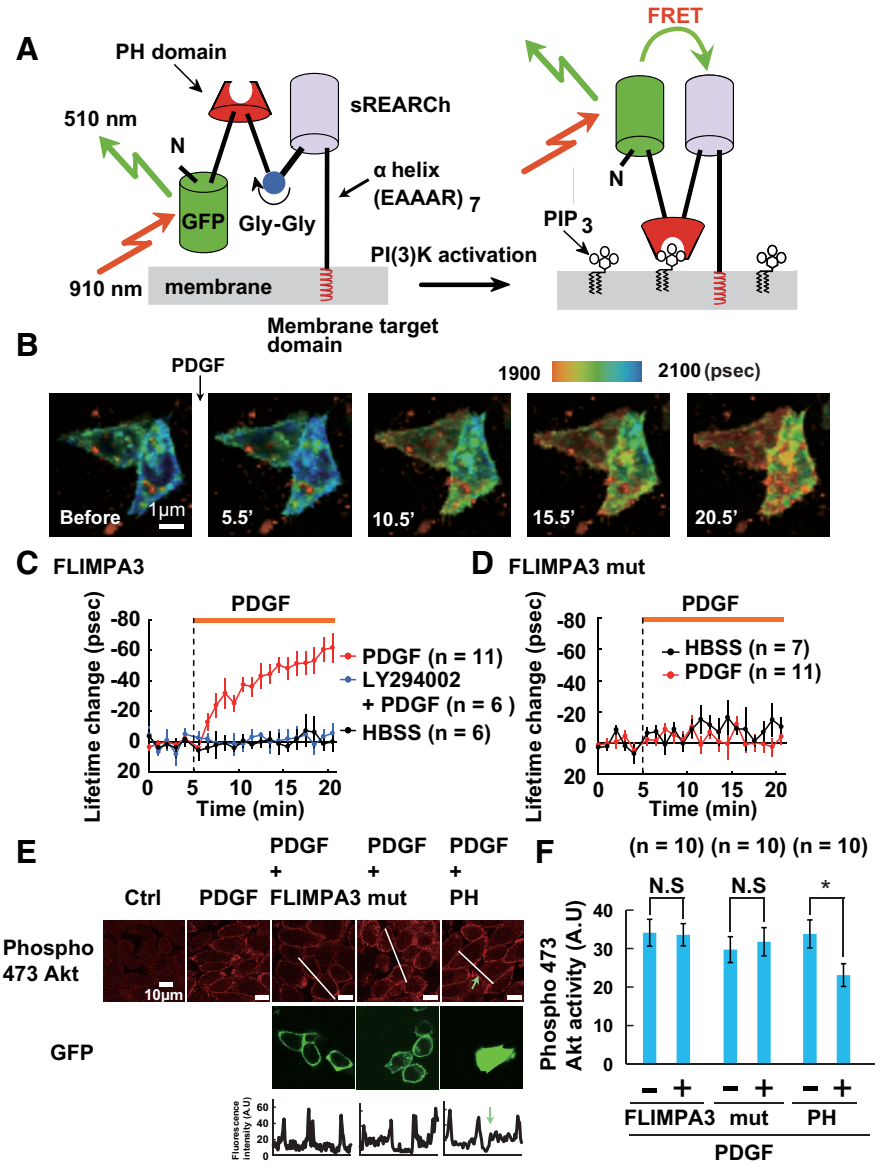

Figure 2. Characterization of FLIMPA3 in living cells. ***A***, Principle of FLIMPA3 for visualizing PIP_3. PIP_3 production induces a conformational change in FLIMPA3 through the binding of the PH domain to PIP_3, leading to an increase in FRET and a decrease in fluorescence lifetime. ***B***, Fluorescence lifetime image of FLIMPA3 in PDGFR-expressed CHO cells. A color gradient was used to represent PIP_3 levels, with a warmer color indicating a shorter fluorescence lifetime and higher PIP_3 levels. The images before (0 min), and 5.5, 10.5, 15.5, and 20. 5 min after addition of 50 ng/ml PDGF were shown. Scale bar, 1 μm. ***C***, Time course of the fluorescence lifetime change of FLIMPA3 in CHO cells after the addition of HBSS, or 50 ng/ml PDGF with or without pre-incubation with 100 μM LY294002. ***D***, Time course analysis of the fluorescence lifetime change of FLIMPA3 mutant in CHO cells after administration of HBSS or 50 ng/ml PDGF. ***E***, ***F***, Effect of FLIMPA3 on PIP_3 signaling assessed by PDGF-induced Akt phosphorylation. Akt phosphorylation at serine residue 473 was detected with Alexa 555-conjugated anti-phospho 473 antibody. Bottom, Indicates immunostaining signal taken from white lines in top.

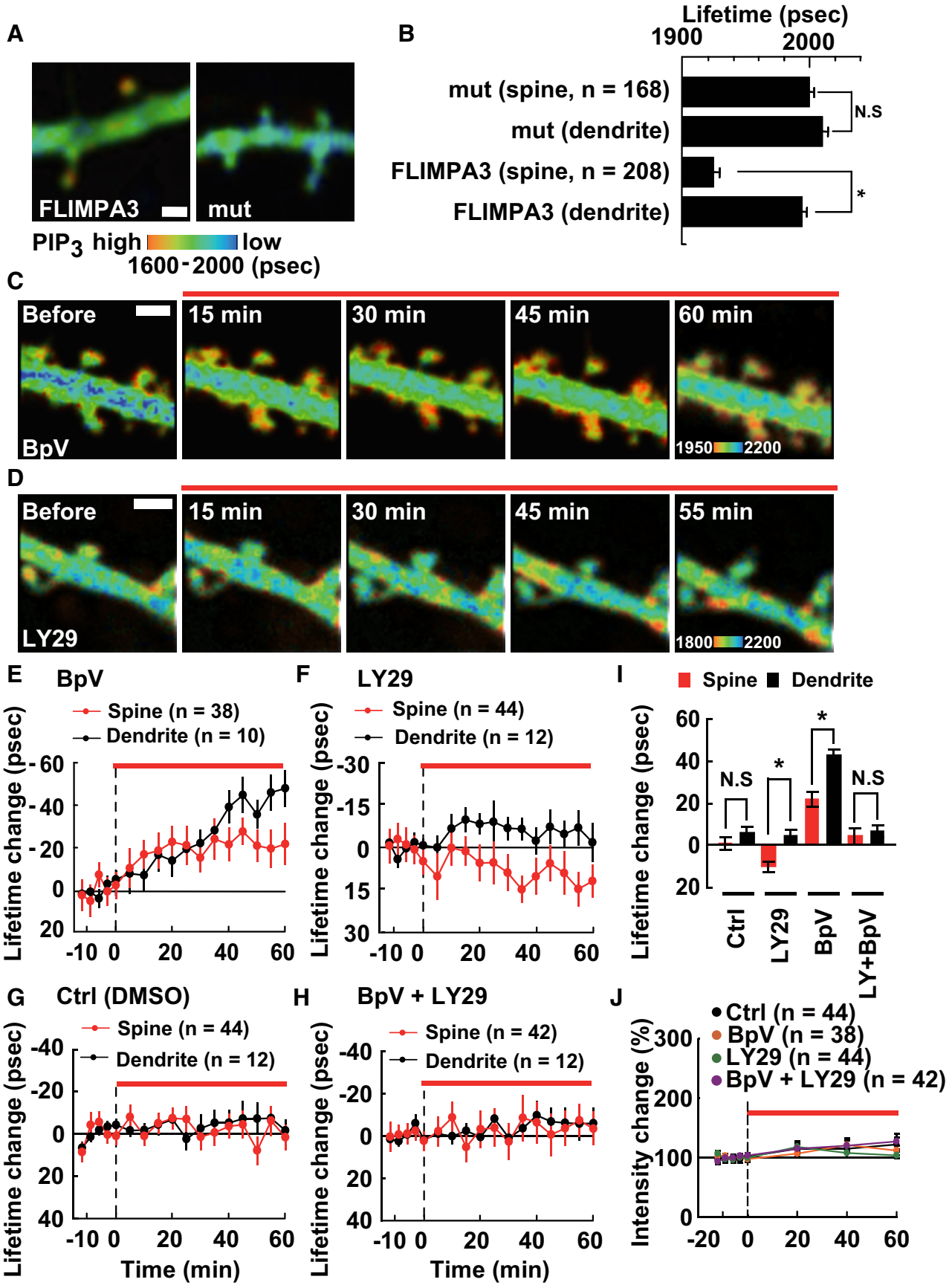

Figure 3. PIP_3 accumulation in spines at static state. ***A***, Fluorescence lifetime imaging of FLIMPA3 and FLIMPA3 mutant (R284CK343A), where PIP_3 binding was abolished. A color gradient was used to represent PIP_3 levels with a warmer color indicating a shorter fluorescence lifetime and higher PIP_3 levels. Scale bar, 1 μm. ***B***, Asterisk denotes a statistically significant difference between the fluorescence lifetime of spines and dendritic shafts of FLIMPA3 ($p < 0.05$); *n* means the number of spines. The number of neurons observed is 25 and 12 in (*Figure legend continues.*)

spinules compared with that observed in control cells during the late phase (Fig. 1*C*,*E*,*F*). To check that PIP_3 itself regulates spinule formation, the effect of PIP_3 masking with overexpressed PH domain, which selectively binds to PIP_3, on spinule formation was examined. As shown in Figure 1, *G* and *H*, the overexpression of a PH domain decreased spinule formation in the early and late phase. Together, these data indicate that PIP_3 regulates spinule formation.

Given that the local accumulation of PIP_3 is crucial for its functions, we decided to investigate the subcellular distribution of PIP_3. We constructed a fluorescence lifetime-based PIP_3 probe, FLIMPA3 (Fig. 2*A*). The probe was based on the ratiometric FRET-based PIP_3 probe, Fllip (Sato et al., 2003). However, the donor CFP and acceptor YFP molecules were exchanged with mEGFP and sREACh, respectively. A PH domain from GRP1 was flanked by mEGFP and sREACh through rigid α-helical linkers consisting of repeated EAAAR sequences. Within one of the rigid linkers, a single diglycine motif was introduced as a hinge. The CAAX box sequence of N-ras was used to target this probe to the plasma membrane (Resh, 1996). When the PH domain binds to PIP_3, a conformational change in the probe occurs through the flexible diglycine motif. This conformational change in the probe causes intramolecular FRET between mEGFP to sREACh, allowing detection of PIP_3 concentration under two-photon fluorescence lifetime imaging microscopy.

First, the response of FLIMPA3 to a physiological stimulation known to increase PIP_3 concentration was examined in non-neuronal cells. FLIMPA3 was expressed in CHO cells expressing PDGF receptor (PDGFR). PDGF treatment promotes the dimerization of PDGFR monomers, resulting in its activation and the phosphorylation of multiple tyrosine residues of PDGFR. PI3K is recruited to these tyrosyl phosphorylation sites through its Src-homology 2 domain, resulting in its activation. When 50 ng/ml PDGF was added to a cell expressing FLIMPA3, fluorescence lifetime decreased immediately and reached a plateau within 20 min (Fig. 2*B*,*C*). Pretreatment of cells with 100 μM LY294002 abolished the decrease in fluorescence lifetime after PDGF stimulation (Fig. 2*C*), indicating that the fluorescence lifetime change occurs through PI3K. Addition of a vehicle (HBSS) did not generate a change in fluorescence lifetime (Fig. 2*C*). A FLIMPA3 mutant, where amino acids R284 and K343 were, respectively, mutated into cysteine and alanine residues to abolish PIP_3 binding, did not generate any signal in response to PDGF stimulation (Fig. 2*D*), indicating that FLIMPA3 responds to PIP_3 through the PH domain. Additionally we confirmed that FLIMPA3 does not perturb PIP_3 signaling by monitoring PDGF-induced Akt activation. Stimulation of CHO cells with PDGF-induced recruitment of Akt to the plasma membrane through PIP_3 binding. This lead to the subsequent phosphorylation of Akt at serine 473 by 3-phosphoinositide-dependent kinase 2 as previously reported (Downward, 1998) (Fig. 2*E*). There was no difference in Akt accumulation between FLIMPA3-expressing cells and neighboring cells, which did not express FLIMPA3, whereas phospho-Akt accumulation was reduced in the cells expressing the PH domain (Fig. 2*E*,*F*). FLIMPA3 mutant also did not perturb Akt activation (Fig. 2*E*,*F*). Together, FLIMPA3 en-

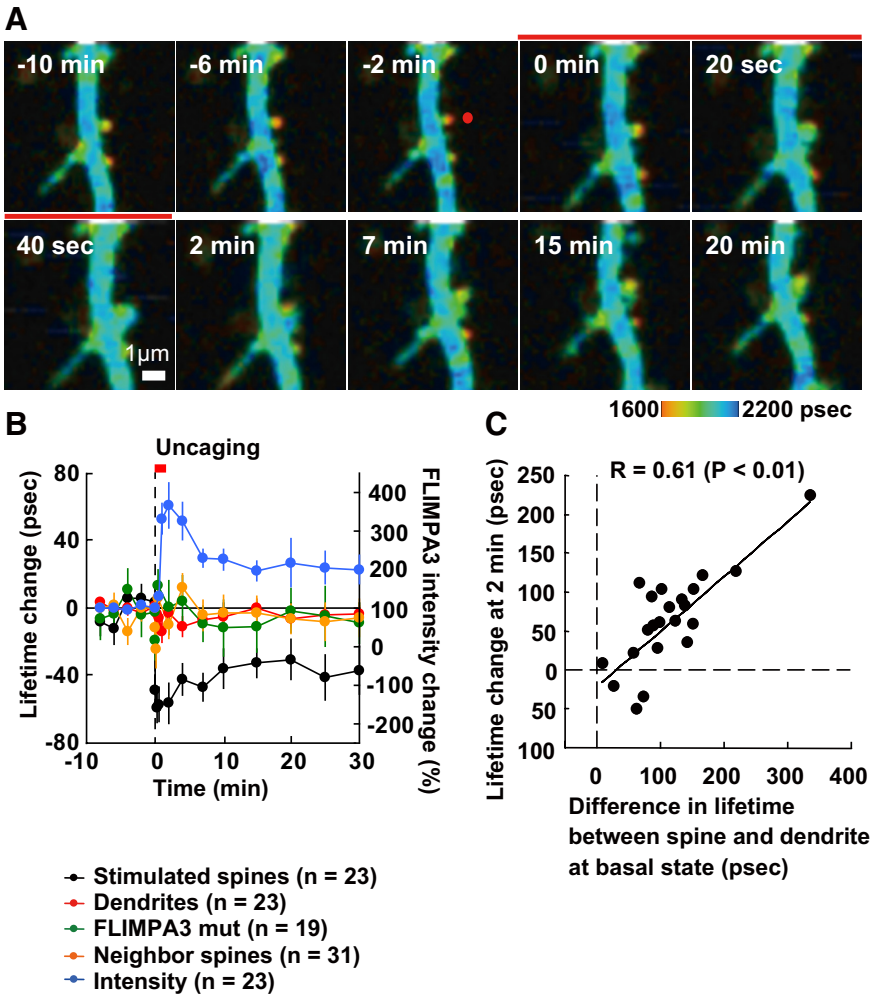

Figure 4. Spatiotemporal dynamics of PIP_3 in spines subjected to sLTP. ***A***, Fluorescence lifetime imaging of FLIMPA3 during sLTP of a single spine induced by two-photon glutamate uncaging. The red spot in the −2 min image indicates the location of the uncaging laser point. White scale bar, 1 μm. The red line indicates the time period of glutamate uncaging. ***B***, Time course of fluorescence lifetime change of FLIMPA3 in a spine subjected to glutamate uncaging, a neighboring spine (within 5 μm of the stimulated spine), and a region of the dendritic shaft next to the stimulated spine. The time course of FLIMPA3 mutant was also shown; *n* indicates the number of spines. The red line indicates the time of glutamate uncaging. Time course of FLIMPA3 intensity change in spines is shown on the right *y*-axis. ***C***, Relationship between PIP_3 concentration at the 2 min time point (*y*-axis) and basal PIP_3 enrichment at basal state. The linear regression line is shown.

←

(*Figure legend continued.*) FLIMPA3 and FLIMPA3 mutant, respectively. ***C***, ***D***, Fluorescence lifetime imaging of PIP_3 after addition of PTEN inhibitor, BpV(HOpic), and PI3K inhibitor, LY294002. Drugs were administered during the period indicated by the red line. Scale bar, 1 μm. ***E–H***, Time course of the fluorescence lifetime change of FLIMPA3 in spines and dendritic shafts after addition of 1 μM BpV(HOpic), 30 μM LY294002, 0.4% DMSO (Ctrl), or 1 μM BpV(HOpic) and 30 μM LY294002. ***I***, The fluorescence lifetime change averaged >40–60 min. N.S., Not significant. Asterisks denote a statistically significant difference ($p < 0.05$). ***J***, Time course of the change in spine size based on FLIMPA3 intensity after the addition of each inhibitor.

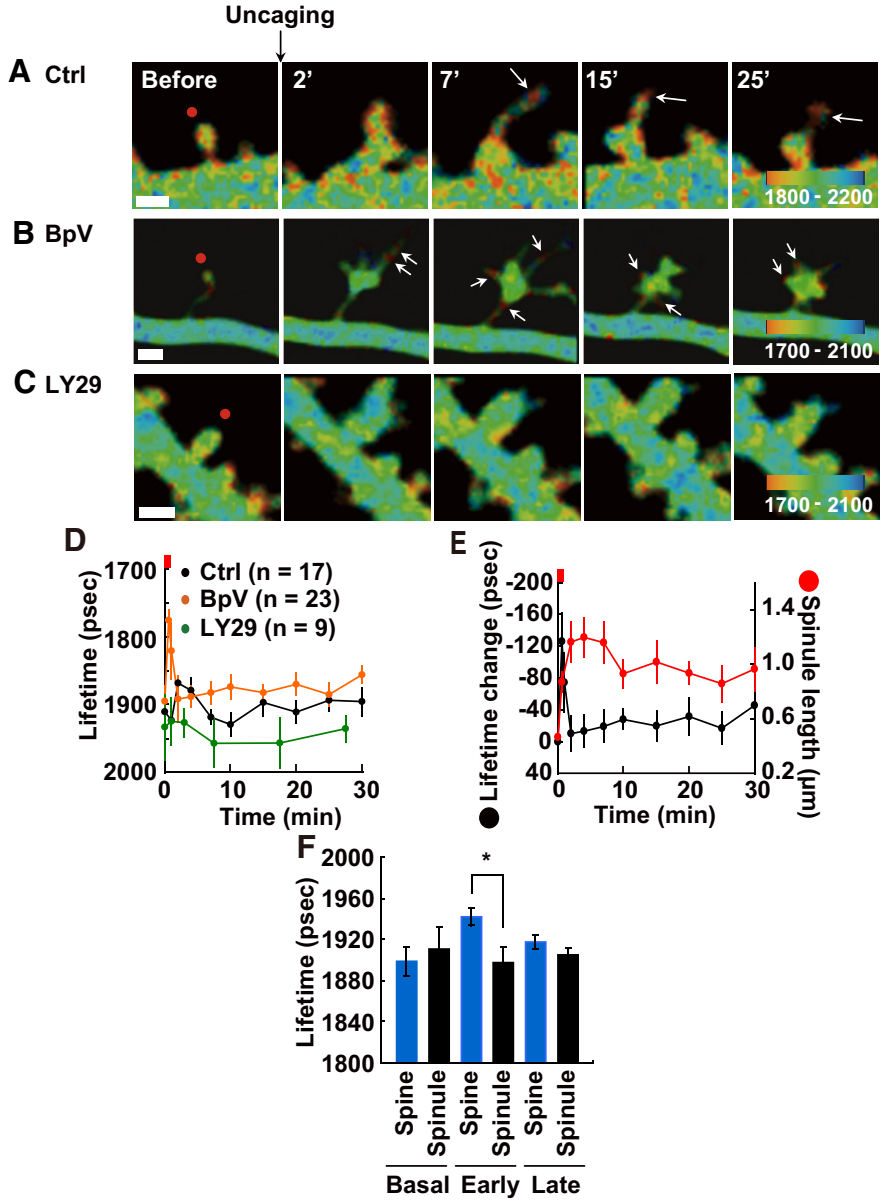

Figure 5. Subspine PIP_3 imaging following sLTP stimulation. ***A–C***, Subspine distribution of PIP_3 by fluorescence lifetime imaging during sLTP (Ctrl 0.4% DMSO (***A***), 1 μM BpV(HOpic) (***B***), and 30 μM LY294002 (***C***), each drug was added >30 min before glutamate uncaging). Red spots on baseline images show the points that were subjected to glutamate uncaging. Arrows show PIP_3 accumulation in spinules. Scale bar, 1 μm. ***D***, Time course of PIP_3 change in spinules; n = number of spines. The red bar indicates the time period of glutamate uncaging. In the case of LY294002, 7–10, 15–20, and 25–30 min, were averaged out due to the smaller dataset. ***E***, Comparison between fluorescence lifetime change in FLIMPA3 (black line) and spinule length (red line) after sLTP in spines pre-incubated with BpV(HOpic). ***F***, Fluorescence lifetime of spinules and spines that exhibit spinules during sLTP was averaged during the early phase and the late phase. Asterisks denote a statistically significant difference ($p < 0.05$).

ables us to detect PIP_3 under physiological conditions without perturbing PIP_3 dynamics.

Next, FLIMPA3 was expressed in CA1 pyramidal neurons of organotypic hippocampal slices (Fig. 3*A*). The fluorescence lifetime image shows that the color in spines is warmer than that observed in the dendritic shaft, indicating an accumulation of PIP_3 in spines. The difference in the fluorescence lifetime between spines and dendritic shafts was significantly larger in cells expressing FLIMPA3 than that in cells with the FLIMPA3 mutant (Fig. 3*B*). These data suggest that PIP_3 accumulated in spines.

To investigate the molecular mechanisms controlling PIP_3 accumulation in spines, the roles of PI3K and PTEN were examined. When neurons were incubated with a PTEN inhibitor, PIP_3 gradually increased (Fig. 3*C*). Data analysis showed that the increase in PIP_3 in dendritic shafts was larger than that in spines, indicating that PTEN activity in dendritic shafts was higher than that in spines (Fig. 3*E*,*I*). The increase in PIP_3 caused by PTEN inhibitor treatment was abolished by pre-incubation with a PI3K inhibitor (Fig. 3*H*,*I*). These results are consistent with previous reports where endogenous levels of PTEN were mainly detected in dendritic shafts (Kreis et al., 2010). There are several factors that explain why the increase in PIP_3 levels was slow. The drug may be slow to diffuse through hippocampal slices. Also, BpV(HOpic) is a metal-containing compound, which may be slow to penetrate the cell membrane. Alternatively, the activity of PI3K in unstimulated cells may be low.

Next, the effect of a PI3K inhibitor on PIP_3 level was examined. After the addition of a PI3K inhibitor, PIP_3 gradually decreases in spines but not in dendritic shafts (Fig. 3*D*,*F*,*I*), suggesting that PI3K is more active in spines than in dendritic shafts. It has been reported that although endogenous PI3K is localized to both spines and dendritic shafts, only PI3K associated with AMPARs that predominantly reside in spines are functionally active (Man et al., 2003), which support our results. Control experiments where dimethylsulfoxide (DMSO) was administered did not reveal any changes in the spines or dendritic shafts (Fig. 3*G*,*I*). Spine size was not affected by the inhibitors when applied 60 min after sLTP stimulation (Fig. 3*J*). Together, these data suggest that the subcellular distribution of PIP_3 is controlled by PTEN and PI3K activity.

Next we investigated the PIP_3 dynamics of single spines during sLTP. Soon after the induction of sLTP, the spine volume became larger and fluorescence lifetime was prolonged. After the initial phase of sLTP, the image no longer became warmer and reached a plateau by 30 min (Fig. 4*A*). The fluorescence lifetime imaging color in dendritic shafts and neighboring spines did not change during sLTP (Fig. 4*B*). No change in fluorescence lifetime color was observed in spines expressing the mutant FLIMPA3 (Fig. 4*B*). Next, the mechanism by which fluorescence lifetime color became blue during sLTP was investigated. The time course curve of FLIMPA3 intensity was well matched with the time course of the change in fluorescence lifetime image color (Fig. 4*B*). Next, the decrease in fluorescence lifetime image color at 2 min after sLTP induction and basal PIP_3 enrichment in spines were assessed. The correlation coefficient is 0.61 ($n = 23$, $p < 0.01$) (Fig. 4*C*). These data indicate that PIP_3 levels in the spine were diluted by a supply of membrane from the dendritic shaft, where there are relatively low levels of PIP_3.

To investigate PIP_3 dynamics in spinules, subspine PIP_3 was examined. PIP_3 accumulation in spinules was observed (Fig. 5*A*,*B*, white arrows). Time course analysis of spinules showed that PIP_3 transiently increased during the early phase and gradually increased ~25–30 min of the late phase (Fig. 5*D*). In spines that were pre-incubated with a PTEN inhibitor, PIP_3 increased more rapidly than in control spines (Fig. 5*B*,*D*). PI3K inhibitor treatment reduced PIP_3 accumulation in spinules at both early and late phases (Fig. 5*C*,*D*). To explore the mechanism by which PIP_3 concentration decreases during the late phase in the presence of a PTEN inhibitor, time course analysis of spinule length was conducted. The length of spinules extended quickly after sLTP induction and peaked at 4 min (Fig. 5*E*, red line). These data suggest that the rapid decrease in PIP_3 concentration is caused by the dilution of PIP_3 due to spinule elongation. PIP_3 levels in spinules showed a massive increase during the early phase compared with that in spines during sLTP (Fig. 5*F*). Together, we have demonstrated that PIP_3 accumulates specifically in spinules, while displaying a decrease in PIP_3 in the whole spine.

Discussion

In the present study, the effect of PIP_3 on spinule formation during sLTP was investigated. The occurrence of spinule formation on spines was increased in a PIP_3-dependent manner. We visualized PIP_3 in single dendritic spines using a fluorescence lifetime-based PIP_3 probe, FLIMPA3. PIP_3 accumulated in spines more than in dendritic shafts. During sLTP of single spines, the high levels of PIP_3 in spines were diluted by an influx of membrane from the dendritic shaft, which has relatively low PIP_3 levels. Subspine imaging revealed that PIP_3 accumulated in spinules, even though PIP_3 in the whole spine region was reduced.

Spinules are induced by a variety of stimulations and their presence is highly variable in different experimental systems. The length of spinules reaches 80–500 nm, at 1 min after high potassium stimulation (Tao-Cheng et al., 2009), 1200 nm at 8 min after local glutamate application (Richards et al., 2005) and 167 nm at 30 min following theta burst stimulation (Toni et al., 1999). Our data showed that the length of spinules reached 880 nm at 4 min after glutamate uncaging under control conditions. Using electron microscopy, spinules are found on 32% of spines under basal conditions in adult male rats (Spacek and Harris, 2004), whereas in the present study, spinules are observed on 1.2% of spines expressing GFP. The discrepancy may be explained by differences in the age of rats, rats used, and experimental conditions.

When PIP_3 levels are modulated by PI3K and PTEN inhibitors, the level of PIP_2 also stoichiometrically change in an opposing way, indicating that there is a possibility that PIP_2 regulates spinule formation. However, considering that the levels of PIP_2 are >100-fold more abundant than PIP_3 levels, the change in PIP_3 levels by PTEN or PI3K probably only makes a small contribution to the change in total PIP_2 levels (Pettitt et al., 2006; Clark et al., 2011). To further strengthen this idea, we performed an experiment to examine the effect of PIP_3 masking with overexpressed PH domain on spinule formation (Fig. 1*G*,*H*), similarly to the approach used by Arendt et al. (2010)to examine the effect of PIP_3 on functional LTP. Overexpression of PH domain affected the early and late phase of spinule formation. These data suggest that PIP_3 regulates the spinule formation. The major difference in the action of overexpressed PH domain versus PI3K inhibitor, which only inhibited spinule formation in the later phase, is whether they affect basal levels of PIP_3 or not. PI3K inhibitor treatment blocks PI3K enzymatic activity but the basal levels of PIP_3 remains constant, at least acutely (change of <10 ps in lifetime after 30 min treatment, which is statistically insignificant; Fig. 3*F*). In contrast, the PH domain can mask all available PIP_3. We speculate that this distinction causes the phenotypic difference between these two treatments. However, the possibility that there may be a PI3K-independent effect during the early phase cannot be totally ruled out.

PIP_3 accumulated in spines more than dendritic shafts (Fig. 3*A*). PIP_3 accumulation was caused by a difference in the local activity of PTEN and PI3K (Fig. 3*C*–*I*). Several papers have examined the unique activity patterns and the distribution of the enzymes. PTEN accumulates at the center of growth cones of dorsal root ganglion cells under basal conditions and subsequently moves to the peripheral membrane during Semaphorin 3A-induced growth cone collapse (Chadborn et al., 2006). In PC12 cells, PTEN is confined to small membrane patches in the cell periphery through the interaction with Myosin Va (van Diepen et al., 2009). In hippocampal CA1 pyramidal neurons, PTEN is localized to dendritic shafts, but not spines (Kreis et al., 2010). Whereas PI3K is evenly distributed throughout a neuron, only PI3K associated with AMPARs that predominantly reside in spines is functionally active during the static state (Man et al., 2003). Thus, the subcellular distribution of PIP_3 is strictly regulated by the location of associated enzymes.

Locally regulated PIP_3 exerts its functions *in situ*. In axons, microdomains of PIP_3 are crucial for driving the formation of axonal F-actin patches, filopodia, and axon branches (Ketschek and Gallo, 2010). Our data showed that after sLTP induction, PIP_3 concentration at spinules increases whereas the concentration in the whole spine decreases, especially during the early phase (Figs. 4, 5). Although PIP_3 concentration in spinules decreases to some extent at the late phase compared with the early phase (Fig. 5*D*), considering that spines are rich in PIP_3 compared with dendritic shaft (Fig. 3*A*), PIP_3 exists in spinules. Based on this result, some possibilities for the biological significance of spinules can be proposed. PIP_3 can be sent to the presynaptic site and may act as a messenger molecule for retrograde signaling. Alternatively PIP_3 signaling may occur at spinules to enable new synapses to form with functional presynaptic boutons, contributing to the change in synaptic connectivity.

References

Arendt KL, Royo M, Fernández-Monreal M, Knafo S, Petrok CN, Martens JR, Esteban JA (2010) PIP3 controls synaptic function by maintaining AMPA receptor clustering at the postsynaptic membrane. Nat Neurosci 13:36–44. CrossRef Medline

Chadborn NH, Ahmed AI, Holt MR, Prinjha R, Dunn GA, Jones GE, Eickholt BJ (2006) PTEN couples Sema3A signalling to growth cone collapse. J Cell Sci 119:951–957. CrossRef Medline

Clark J, Anderson KE, Juvin V, Smith TS, Karpe F, Wakelam MJ, Stephens LR, Hawkins PT (2011) Quantification of PtdInsP3 molecular species in cells and tissues by mass spectrometry. Nat Methods 8:267–272. CrossRef Medline

Downward J (1998) Mechanisms and consequences of activation of protein kinase B/Akt. Curr Opin Cell Biol 10:262–267. CrossRef Medline

Gu J, Tamura M, Pankov R, Danen EH, Takino T, Matsumoto K, Yamada KM (1999) Shc and FAK differentially regulate cell motility and directionality modulated by PTEN. J Cell Biol 146:389–403. CrossRef Medline

Han J, Luby-Phelps K, Das B, Shu X, Xia Y, Mosteller RD, Krishna UM, Falck JR, White MA, Broek D (1998) Role of substrates and products of PI 3-kinase in regulating activation of Rac-related guanosine triphosphatases by Vav. Science 279:558–560. CrossRef Medline

Innocenti M, Frittoli E, Ponzanelli I, Falck JR, Brachmann SM, Di Fiore PP, Scita G (2003) Phosphoinositide 3-kinase activates Rac by entering in a

complex with Eps8, Abi1, and Sos-1. J Cell Biol 160:17–23. CrossRef Medline

Jaworski J, Spangler S, Seeburg DP, Hoogenraad CC, Sheng M (2005) Control of dendritic arborization by the phosphoinositide-3′-kinase-Akt-mammalian target of rapamycin pathway. J Neurosci 25:11300–11312. CrossRef Medline

Jurado S, Benoist M, Lario A, Knafo S, Petrok CN, Esteban JA (2010) PTEN is recruited to the postsynaptic terminal for NMDA receptor-dependent long-term depression. EMBO J 29:2827–2840. CrossRef Medline

Ketschek A, Gallo G (2010) Nerve growth factor induces axonal filopodia through localized microdomains of phosphoinositide 3-kinase activity that drive the formation of cytoskeletal precursors to filopodia. J Neurosci 30:12185–12197. CrossRef Medline

Kreis P, van Diepen MT, Eickholt BJ (2010) Regulation of PTEN in neurons by myosin-based transport mechanisms. Adv Enzyme Regul 50:119–124. CrossRef Medline

Man HY, Wang Q, Lu WY, Ju W, Ahmadian G, Liu L, D'Souza S, Wong TP, Taghibiglou C, Lu J, Becker LE, Pei L, Liu F, Wymann MP, MacDonald JF, Wang YT (2003) Activation of PI3-kinase is required for AMPA receptor insertion during LTP of mEPSCs in cultured hippocampal neurons. Neuron 38:611–624. CrossRef Medline

Matsuzaki M, Honkura N, Ellis-Davies GC, Kasai H (2004) Structural basis of long-term potentiation in single dendritic spines. Nature 429:761–766.

Murakoshi H, Lee SJ, Yasuda R (2008) Highly sensitive and quantitative FRET-FLIM imaging in single dendritic spines using improved non-radiative YFP. Brain Cell Biol 36:31–42. CrossRef Medline

Oikawa T, Yamaguchi H, Itoh T, Kato M, Ijuin T, Yamazaki D, Suetsugu S, Takenawa T (2004) PtdIns(3,4,5)P3 binding is necessary for WAVE2-induced formation of lamellipodia. Nat Cell Biol 6:420–426. CrossRef Medline

Pettitt TR, Dove SK, Lubben A, Calaminus SD, Wakelam MJ (2006) Analysis of intact phosphoinositides in biological samples. J Lipid Res 47:1588–1596. CrossRef Medline

Resh MD (1996) Regulation of cellular signalling by fatty acid acylation and prenylation of signal transduction proteins. Cell Signal 8:403–412. CrossRef Medline

Richards DA, Mateos JM, Hugel S, de Paola V, Caroni P, Gähwiler BH, McKinney RA (2005) Glutamate induces the rapid formation of spine head protrusions in hippocampal slice cultures. Proc Natl Acad Sci U S A 102:6166–6171. CrossRef Medline

Sato M, Ueda Y, Takagi T, Umezawa Y (2003) Production of PtdInsP3 at endomembranes is triggered by receptor endocytosis. Nat Cell Biol 5:1016–1022. CrossRef Medline

Shinohara M, Terada Y, Iwamatsu A, Shinohara A, Mochizuki N, Higuchi M, Gotoh Y, Ihara S, Nagata S, Itoh H, Fukui Y, Jessberger R (2002) SWAP-70 is a guanine-nucleotide-exchange factor that mediates signalling of membrane ruffling. Nature 416:759–763. CrossRef Medline

Spacek J, Harris KM (2004) Trans-endocytosis via spinules in adult rat hippocampus. J Neurosci 24:4233–4241. CrossRef Medline

Tao-Cheng JH, Dosemeci A, Gallant PE, Miller S, Galbraith JA, Winters CA, Azzam R, Reese TS (2009) Rapid turnover of spinules at synaptic terminals. Neuroscience 160:42–50. CrossRef Medline

Thomas CC, Dowler S, Deak M, Alessi DR, van Aalten DM (2001) Crystal structure of the phosphatidylinositol 3,4-bisphosphate-binding pleckstrin homology (PH) domain of tandem PH-domain-containing protein 1 (TAPP1): molecular basis of lipid specificity. Biochem J 358:287–294. CrossRef Medline

Toni N, Buchs PA, Nikonenko I, Bron CR, Muller D (1999) LTP promotes formation of multiple spine synapses between a single axon terminal and a dendrite. Nature 402:421–425. CrossRef Medline

van Diepen MT, Parsons M, Downes CP, Leslie NR, Hindges R, Eickholt BJ (2009) MyosinV controls PTEN function and neuronal cell size. Nat Cell Biol 11:1191–1196. CrossRef Medline